Journal of Nuclear Materials 393 (2009) 459–464

Contents lists available at ScienceDirect

Journal of Nuclear Materials

journal homepage: www.elsevier.com/locate/jnucmat

Determination of the activity coefficient of Am in liquid Al by electrochemical methods

G. De Córdoba [a,*], A. Laplace [b], O. Conocar [b], J. Lacquement [b]

[a] HLW/DFN/DE, CIEMAT, Avda, Complutense 22, Madrid 28040, Spain
[b] DEN/DRCP/SCPS/LPP, CEA, Site de Marcoule, Bât. 399 – BP 17171, 30207 Bagnols sur Cèze, France

ARTICLE INFO

Article history:
Received 30 January 2009
Accepted 6 July 2009

Keywords:
Americium
Aluminium
Activity coefficient
Molten chlorides
Cyclic voltammetry

ABSTRACT

The activity coefficient of americium in liquid aluminium has been determined by electrochemical methods. To the author's knowledge, this is the first time this value is published in the open literature. For radiation safety reasons only 100 mg of this highly radioactive element were permitted to be manipulated inside the glove-box. Hence an "ad hoc" experimental set-up, which allows working with small amounts of solvent, has been designed. The Am(III) solution has been prepared by direct AmO_2 dissolution into $CaCl_2$–NaCl; the conversion into its chloride form has been achieved by carbochlorination (Cl_2 + C) at 600 °C. Cyclic voltammetry technique, performed in the obtained $CaCl_2$–NaCl–$AmCl_3$ solution, has allowed a first estimation for the logarithm of the activity coefficient, being equal to $\log \gamma_{Am(Al)} = -6.7 \pm 1$ at 700 °C.

1. Introduction

Actinide recycling by separation and transmutation is considered worldwide as a promising strategy for an efficient use of the nuclear fuel as well as for nuclear waste minimization, thus contributing to make nuclear energy sustainable. With this purpose, two major fuel reprocessing technologies have been explored so far to separate actinides (An) from fission products (FP) arising from nuclear energy production: hydrometallurgical and pyrometallurgical processes.

Pyrochemical processes are currently being investigated as an alternative option to the well-known aqueous reprocessing since they offer some potential advantages. Among them, high radiation stability of salts and metallic phases used as solvents stands out. As the nuclear fuels proposed in the future innovative reactor systems will reach high burn-ups and will contain significant amounts of minor actinides (Np, Am and Cm), pyrometallurgical technology appears to be an attractive option for fuel reprocessing [1].

The techniques identified to carry out pyrochemical separation between An and FP are molten salt–liquid metal reductive extraction in molten fluoride media and electro-deposition on a solid or liquid metal electrode in molten chlorides [2]. Special attention is devoted to lanthanide fission products (Ln) since their similar chemical behaviour to An makes their separation difficult.

The selectivity of a given extraction process can be estimated with the aid of thermodynamic equilibrium constants and the activity coefficients which give an idea of the interactions between the elements and the molten salt or liquid metal phases [3].

In the liquid–liquid extraction in a metallic solvent (Me) the expression of the logarithm of the separation factor ($S_{An/Ln}$) is as follows [4]:

$$\log S_{An/Ln} = \log\left(\frac{K^0_{An}}{K^0_{Ln}}\right) + \log\left(\frac{\gamma_{An^{n+}}}{\gamma_{Ln^{n+}}}\right) + \log\left(\frac{\gamma_{Ln(Me)}}{\gamma_{An(Me)}}\right) \quad (1)$$

where K^0_i is the standard thermodynamic constant of the extraction equilibrium for An or Ln and γ_i is the activity coefficient of i in the salt phase or in the metallic solvent (Me) when specified.

The An/Ln electrolytic extraction process is controlled by the equilibrium potential difference between the redox systems Ln^{n+}/Ln and An^{n+}/An calculated by applying the Nernst law. The expression obtained is quite similar to equation (1).

Whatever the technique selected, the An/Ln separation is controlled by the standard free energy differences for pure compounds (or standard potentials), the activity coefficients ratio in the salt phase ($\gamma_{An^{n+}}/\gamma_{Ln^{n+}}$) and the activity coefficients ratio in the metallic phase ($\gamma_{Ln(Me)}/\gamma_{An(Me)}$). In the particular case of the activity coefficient ratio in the metallic phase this can vary a lot both between An and Ln for the same metallic solvent and between different metallic solvents for the same element [5,6]. Hence, the choice of the metallic solvent is crucial for the separation process.

Thermodynamic calculations and laboratory scale experiments in fluoride and chloride media indicate that Al is the most promis-

* Corresponding author. Tel.: +34 91 346 0841; fax: +34 91 346 6233.
E-mail address: guadalupe.cordoba@micinn.es (G. De Córdoba).

0022-3115/$ - see front matter © 2009 Elsevier B.V. All rights reserved.
doi:10.1016/j.jnucmat.2009.07.002

ing metallic solvent to support the selective An recovery and separation from Ln, both by electrolytic and chemical extraction processes [7,8]. In this sense, the knowledge of activity coefficients in Al of the elements of interest (mainly An and Ln) is considered a necessary tool since they will allow modelling the different pyrochemical processes envisaged.

A compilation of activity coefficients for the An and several FP in different metallic phases is reported in the literature [5]. It is found that U, Th and Ln elements have been widely studied. However, the actinides Pa, Np, Am and Cm have been little investigated or even not studied due to the difficulty for their handling and for obtaining them in pure form [9].

In the case of the Al solvent, only the activity coefficients of Th, U and Pu have been reported [5]. The activity coefficient of Am, Np and Cm have not been published in the literature to date.

This work reports a first estimation of the activity coefficient of Am in liquid Al at 700 °C obtained by cyclic voltammetry. Due to the restrictions for handling this highly radioactive element, an "ad hoc" experimental set-up, which allows working with small amounts of solvent, has been designed. The set-up and methodology have been previously tested and validated by using Nd as an Am surrogate [10].

Basically, the activity coefficient of an element in a metallic phase can be determined by measuring the electromotive force (*emf*) of the galvanic cell: $M_{\text{pure}}/\text{MCl}_n$, *molten salt*$/M_{\text{Me}}$. On the left side, the electrode consists of the pure metal of the element under study (M). On the right side, the electrode is formed by the element M dissolved in a metallic solvent (Me). The electrolyte is a molten salt containing the considered element dissolved as MCl_n (if the study is done in chloride media) at a known concentration. The logarithm of the activity coefficient is related to the *emf* between pure metal and alloyed metal through the following expression:

$$\log \gamma_{\text{M(Me)}} = \frac{n \cdot F \cdot emf}{2.3RT} - \log X_{\text{M(Me)}} \quad (2)$$

being $emf = E_{\text{eq}(\text{M}^{n+}/\text{M})} - E_{\text{eq}(\text{M}^{n+}/\text{M(Me)})}$ where E_{eq} are the equilibrium potentials of the M^{n+}/M and $\text{M}^{n+}/\text{M(Me)}$ systems (V), R is the ideal gas constant (J/mol K), T is the absolute temperature (K), F is the Faraday constant (C/mol) and X is the mole fraction of M in the metallic solvent.

2. Experimental

2.1. General

The molten electrolyte used in the experiments was the eutectic mixture CaCl_2–NaCl (52–48 mol%) which was selected due to its high melting point (m.p. = 500 °C) compared to other chloride mixtures like LiCl–KCl (m.p. = 352 °C). This permits working with liquid Al (m.p. = 660 °C) and helps minimizing the solvent evaporation. In any case, some evaporation of the chloride solvent is expected at the temperature tested (700 °C).

CaCl_2 (Aldrich, 97%) was previously dehydrated under vacuum (1 mbar) by a progressive heating at 127 °C and 300 °C. NaCl (Aldrich, 99.999%) was not pre-treated. The CaCl_2–NaCl mixture was then purified by HCl (Praxair, 99.995%) bubbling at 600 °C for 60 min to remove any trace of oxygen and moisture. AmCl_3 solution was prepared by direct dissolution of AmO_2 (^{241}Am 100% isotopic composition) in pure CaCl_2–NaCl; the conversion into its chloride form was performed by carbochlorination ($\text{Cl}_2 + \text{C}$) at 600 °C.

The main component of the electrolytic cell was a sealed quartz container resistant to high temperature. The salt mixture was introduced in a glassy carbon (GC) crucible (Sigradur SGL Carbon, H = 85 mm, ∅ = 50–45 mm) which in its turn was placed into a safeguard quartz crucible, then into the quartz cell. The cell was hermetically closed and kept under dry Ar gas flow (Air Liquide, Ar N60, $\text{H}_2\text{O} < 0.6$ ppm, $\text{O}_2 < 0.1$ ppm) during all the experiment. Quartz tubes were used to introduce the Ar and HCl gases into the cell. For the carbochlorination ($\text{Cl}_2 + \text{C}$) test, Cl_2 (Praxair, 99.99%) was introduced through a porous graphite tube (Carbon Lorraine, $\varnothing_{\text{ext-int}}$ = 8–3.5 mm, impurities < 200 ppm) shielded in a quartz tube to avoid the gas leakage. In addition to the graphite tube, three graphite rods (Goodfellow, 99.997%, ∅ = 3 mm) were introduced in the melt to increase the active reaction surface between chlorine and graphite.

The electrochemical set-up enables the use of reduced amounts of salt solvent (30 g); hence, it allows the electrochemical study even if small amounts of solute are used, as it is the case for Am. A boron nitride (BN) crown (MSCE, HIP grade, H = 15 mm, ∅ = 43–11 mm), placed at the bottom of the GC crucible, was used in the experiments. This system presents two main advantages: it allows working with a liquid metal electrode, consisting of a small quartz container with the metal inside and placed in the crown central hole; at the same time, it permits reducing the amount of solvent and thus reaching a higher Am concentration in solution. Fig. 1 shows a picture of the experimental set-up.

The molten salt temperature was controlled by an S-type thermocouple (±1 °C) sheathed into an alumina tube (Sceram, 99.7%) immersed in the molten bath. Thirty grams of salt are approximately 1 cm high in the GC crucible. A temperature gradient around 5 °C/cm of melt was measured. This gradient is taken into account to calculate the uncertainty on the activity coefficient determination.

Am concentration in solution was determined by taking salt samples from the melt. They were dissolved and diluted in HNO_3 (1 M) and subsequently analyzed by the alpha-counting technique.

2.2. Electrodes

For the electrochemical study, two types of working electrodes were used:

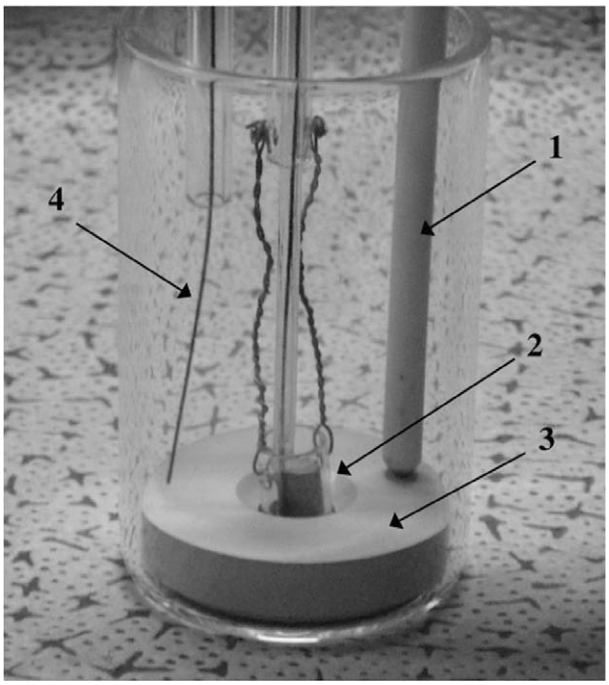

Fig. 1. Picture of the experimental set-up: (1) Reference electrode; (2) Al electrode assembly; (3) BN crown; (4) W electrode. A Pyrex crucible was used to take the picture.

– An inert W wire (Goodfellow, 99.9%, ∅ = 1 mm) to form in situ a pure Am deposit. Before its use the surface was polished thoroughly with sandpaper and then washed with ethanol. The active surface was determined after each experiment by measuring the immersion depth of the electrode in the melt.
– A liquid Al electrode to form Am–Al alloys. It consists of a small quartz container (S = 0.37 cm^2) hold with a Pt wire (Goodfellow, 99.99%, ∅ = 0.5 mm) which in its turn is tied to a quartz tube (see picture in Fig. 1). The electric contact was made of a W wire (Goodfellow, 99.9%, ∅ = 0.5 mm) isolated from the electrolyte. The amount of Al introduced in the container varied from 0.7 to 1 g. Before its use, aluminium (Aldrich, 99.999 + % pellets) was cleaned with acetone.

As reference electrode the AgCl/Ag system was used. It consists of a Ag wire (Goodfellow, 99.99%, ∅ = 1 mm) dipped into a closed-end mullite tube (Haldenwanger, 99.7%) containing a 0.75 mol/kg AgCl (Aldrich, 99%) solution in $CaCl_2$–NaCl [11,12]. The potentials measured against AgCl/Ag were converted into values versus the $Cl_{2(1atm)}/Cl^-$ system. This was made by measuring the Cl_2 gas release potential (oxidation of chloride ions) by cyclic voltammetry on a W electrode. The conversion potential varied between −1.02 and −1.05 V depending on the working temperature.

The auxiliary electrode was made of a W wire (Goodfellow, 99.9%, ∅ = 1 mm) or a graphite rod (Goodfellow, 99.997%, ∅ = 3 mm).

The electrochemical measurements were performed with an Autolab PG Stat 30 (Metrohm) potentiostat–galvanostat, associated to the GPES software. This software was also used to simulate the experimental results. The current–potential curves simulation is based on a finite difference method. Equations of transport of electro-active substances to the electrode surface are solved by the Crank–Nicholson technique [13] and the current is calculated by applying the Butler–Volmer equation [14].

3. Results and discussion

3.1. AmO_2 dissolution

$AmCl_3$ solution was prepared by AmO_2 dissolution by carbochlorination at 600 °C. The reaction that takes place can be written as follows [15]:

$$AmO_{2(s)} + C_{(s)} + 3/2Cl_{2(g)} \rightarrow AmCl_{3(l)} + CO_{2(g)} \quad (3)$$

Thirty grams of $CaCl_2$–NaCl, previously purified by HCl, together with 121 mg of AmO_2 were introduced in the GC crucible and then placed in the quartz cell. The mixture was kept under inert Ar flow during its melting. Carbochlorination was performed by bubbling Cl_2 gas into the melt through a porous graphite tube. The reaction surface between Cl_2 and graphite was increased by introducing three graphite rods in the solution. Cl_2 was bubbled through the melt at a volumetric flow rate of 3 l/h during 50–60 min. Ar was also bubbled above the molten bath. With the purpose of fully replacing the Ar atmosphere in the cell, Cl_2 was bubbled through it during 10–15 min. The reaction cell was then closed and maintained under Cl_2 atmosphere during one night or more. The atmosphere was renewed depending on the evolution of the dissolution reaction. At the end of the carbochlorination, Ar was bubbled through the melt to remove the Cl_2 excess [16].

Dissolution rate was followed by taking samples from the bath. The analysis of the samples showed that a 100% dissolution of the initial AmO_2 (121 mg) was reached. This corresponds to a maximum concentration of americium in solution of 0.014 mol/kg.

3.2. Preliminary study. Bath control by cyclic voltammetry

3.2.1. Inert W electrode

The $CaCl_2$–NaCl–$AmCl_3$ solution obtained by carbochlorination was examined by cyclic voltammetry on solid W and liquid Al electrodes. Fig. 2 shows cyclic voltammograms corresponding to the Am(III) ions reduction on a W electrode at 700 °C. When Am(III) ions are reduced at the W electrode surface two groups of signals are observed (1c-1a; 2c-2a). The cathodic wave 1c at ∼−1.59 V vs. AgCl/Ag is associated to the anodic wave 1a (E_p^A∼ −1.40 V vs. AgCl/Ag); this system has the characteristic shape of a soluble–soluble exchange which is attributed to the Am(III)/Am(II) redox couple. Peak 2c (E_p^A ∼ −2.12 V vs. AgCl/Ag) associated with the anodic peak 2a (E_p^A∼−1.97 V vs. AgCl/Ag) is typical of an exchange involving an insoluble product that is attributed to the Am(II)/Am(0) system. These results are consistent with those reported by other authors on Am behaviour in chloride media [17,18].

The low concentration of Am in solution (0.014 mol/kg max.) and the high working temperature (700 °C), which approach the reduction potentials of both, the solvent (Na(I) → Na(0)) and Am (Am(II) → Am(0)), made it difficult to measure the reduction and oxidation peaks. In addition, the corrosion reaction between metal Am and the solvent, and the one between metal Am and Am(III) ions are expected to occur; these reactions will hinder the *emf* measurements [5,19].

3.2.2. Reactive liquid Al electrode

Cyclic voltammetry on liquid Al electrode was also applied in the $CaCl_2$–NaCl–$AmCl_3$ system, as it is shown in Fig. 3(a). It is found that the available electrochemical window in $CaCl_2$–NaCl at 700 °C (also plotted in Fig. 3b) is significantly smaller (ΔE = 670 mV) than that on inert W (ΔE = 3.57 V). On Al, the cathodic limit is shifted towards more positive values due to the formation of Al–Na alloys (−1.7 V vs. AgCl/Ag). The anodic limit is imposed by the oxidation of the metal Al substrate into Al(III) (−1.03 V vs. AgCl/Ag).

The voltammogram of Fig. 3b shows a single cathodic wave corresponding to the Am(III) reduction into metal Am (E_p^c∼−1.24 V vs. AgCl/Ag), stabilized in liquid Al. The anodic wave, corresponding to the oxidation of metal Am (dissolved in liquid Al) into Am(III) ions, is very difficult to distinguish (E_p^A ∼ −1.06 V vs. AgCl/Ag). This is because it appears at a potential very close to the anodic limit, that is the Al oxidation into Al(III). The low intensity of this wave could be due to the low Am concentration in solution; furthermore, the probable presence of oxides in the molten bath could lead to some metal Am re-oxidation.

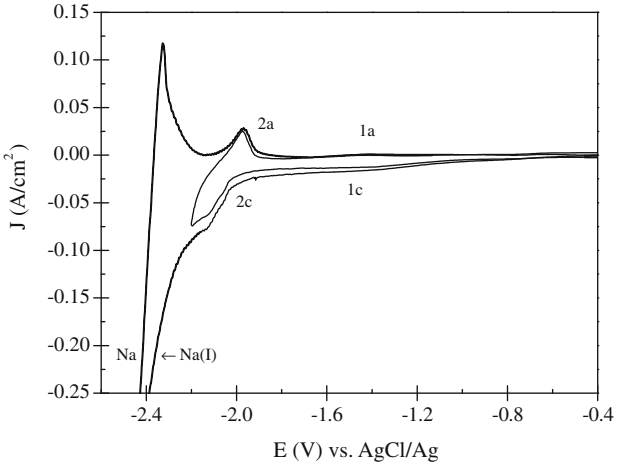

Fig. 2. Cyclic voltammograms in $CaCl_2$–NaCl–$AmCl_3$ (0.014 mol/kg) on W electrode (S = 0.35 cm^2). T = 700 °C, v = 0.1 V/s. Reverse cathodic limits: −2.2, −2.5 V.

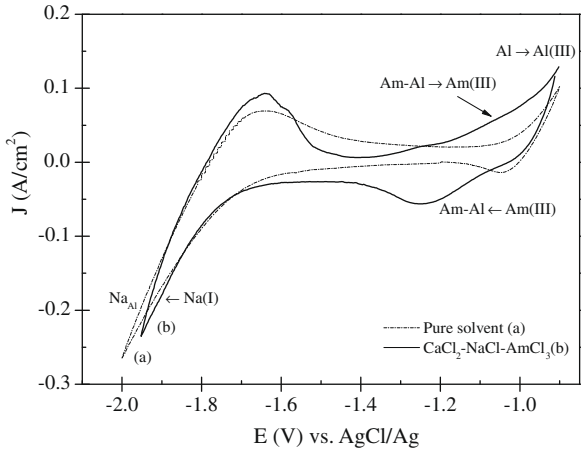

Fig. 3. Cyclic voltammograms of $CaCl_2$–NaCl–$AmCl_3$ on Al(l) ($S = 0.37$ cm^2). Curve (a): [Am] = 0, $v = 0.05$ V/s. Curve (b): [Am] = 0.01 mol/kg, $v = 0.003$ V/s. $T = 700$ °C.

The more anodic reduction potential of Am(III) ions on reactive Al(l) is due to the lowered activity of Am by Al–Am alloys formation. In addition, the stabilization of metal Am in the Al phase by alloys formation shifts equilibrium (4) to the left side. This would avoid any possible corrosion of the metallic deposit in the case of the electrolytic extraction of Am.

$$2\mathrm{Am(III)} + \mathrm{Am} \leftrightarrow 3\mathrm{Am(II)} \tag{4}$$

It has to be noticed that the Am(III)/Am(Al) reduction potential appears well separated from the solvent reduction Na(I)/Na(Al); hence, the electrolytic recovery of Am into Al without co-reduction of the solvent would be feasible.

3.3. Estimation of the activity coefficient by cyclic voltammetry

It has been reported that cyclic voltammetry using liquid metals as working electrodes can be used as an alternative approach to determine thermodynamic data on alloys behaviour, such as the activity coefficient [20]. In order to do so, an essential condition which should be fulfilled is to maintain the Am concentration in the Al phase below its solubility limit, situation at which Am(III)/Am(Al) is considered as a soluble–soluble system.

On the other hand, the particular situation at which the concentrations of Am in the salt and metallic inter-phases are equal ($X_{Am(III)} = X_{Am(Al)}$), is assumed. Taking this into account and applying the Nernst equation, the logarithm of the activity coefficient log $\gamma_{Am(Al)}$ can be expressed as a difference between formal standard potentials as:

$$log\gamma_{Am(Al)} = \frac{3F}{2.3RT}\left(E'^{0}_{Am(III)/Am(0)} - E'^{0}_{Am(III)/Am(Al)}\right) \tag{5}$$

where E'^0 is the formal standard potential (V) of the Am(III)/Am(0) and Am(III)/Am(Al) redox systems.

In order to be able to calculate the activity coefficient of Am in Al(l) from equation (5), it is first necessary to determine the formal standard potentials of the two redox systems Am(III)/Am(0) and Am(III)/Am(Al). This has been done by applying the techniques of cyclic voltammetry and open-circuit potentiometry as it is described below.

3.3.1. Am(III)/Am(0) formal standard potential

The two steps reduction of Am(III) ions into pure metal Am requires the previous determination of the formal standard potential of Am(III)/Am(II) and Am(II)/Am(0) systems. Afterwards, the formal standard potential of Am(III)/Am(0) can be calculated by combining those ones. The working temperatures range tested has been 675–800 °C.

3.3.1.1. Am(III)/Am(II) redox system. The formal standard potential $E'^{0}_{Am(III)/Am(II)}$ has been estimated from the analysis of the cyclic voltammograms registered at several potential scan rates on inert W. In order to do so, some assumptions have been made [18]: (i) the Am(III)/Am(II) exchange behaves as a reversible system (at low scan rates < 0.1 V/s); (ii) the Am(III)/Am(II) and Am(II)/Am(0) systems are separate enough to consider them independent.

The reversible half-wave potential $E_{1/2}$ for the Am(III)/Am(II) system can be calculated from the equation [14]:

$$E_{1/2} = \frac{E_p^c + E_p^A}{2} \tag{6}$$

In its turn, the $E_{1/2}$ is related to the formal standard potential by the following expression:

$$E_{1/2} = E'^{0}_{Am(III)/Am(II)} + \frac{RT}{F}\ln\left(\frac{D_{Red}^{1/2}}{D_{Ox}^{1/2}}\right) \tag{7}$$

where E'^0 is given in the mol/cm^3 scale and the diffusion coefficient is in cm^2/s. It is assumed here that the diffusion coefficient of the reduced Am(II) and oxidized Am(III) species are similar ($D_{Ox} = D_{Red}$), hence it is obtained that $E_{1/2} = E'^0$.

The estimated value of the formal standard potential is equal to $E'^{0}_{Am(III)/Am(II)} = -2.52$ V($\pm$30 mV)vs. $Cl_{2(1\ atm)}/Cl^-$, in the mole fraction scale and at 700 °C. The values obtained at different temperatures are gathered in Table 1. The given uncertainty corresponds to the error (standard deviation) coming from the calculation of the standard potential taking into account the assumption $D_{Ox} = D_{Red}$.

3.3.1.2. Am(II)/Am(0) redox system. The formal standard potential $E'^{0}_{Am(II)/Am(0)}$ has been calculated by using the open-circuit potentiometry technique (ocp). It consists of applying a short cathodic polarization (60–300 s) to form a metallic Am deposit on the W surface. Then, the open-circuit potential of the electrode is registered versus time and it gives access to the equilibrium potential $E_{eq\ Am(II)/Am(0)}$. Fig. 4 shows an ocp curve registered in $CaCl_2$–NaCl–$AmCl_3$ after applying a potential for pure Am deposition on W. It is observed a short potential plateau (−1.94 V vs. AgCl/Ag) associated to the Am(II)/Am(0) exchange from which the pseudo-equilibrium potential was measured. The corrosion reaction between metal Am and Am(III) in solution to form Am(II) ions is expected to occur and it would prevent the formation of stable deposits. This plateau is followed by a slight wave (~−1.78 V vs. AgCl/Ag) that could correspond to a soluble–soluble redox system (Am(III)/Am(II)). In addition, the small waves observed at more positive potentials, before reaching the rest potential of the working electrode, are attributed to the presence of impurities in the melt. Similar waves, in the same potential region, have been observed in the ocp curves for the pure $CaCl_2$–NaCl solvent.

If it is assumed that, at the electrode surface, Am(III) ions have been completely reduced and $[Am(II)]_{electrode} = [Am(III)]_{bulk}$, the

Table 1
Formal standard potential (V) of the Am redox systems in $CaCl_2$–NaCl at different temperatures. Potential values are expressed versus $Cl_{2(1\ atm)}/Cl^-$ and in mole fraction scale.

T (°C)	$E'^{0}_{Am(III)/Am(II)}$	$E'^{0}_{Am(II)/Am(0)}$	$E'^{0}_{Am(III)/Am(0)}$
675	−2.54 ± 0.03	−2.71 ± 0.01	−2.65 ± 0.03
700	−2.52 ± 0.03	−2.70 ± 0.006	−2.64 ± 0.02
750	−2.51 ± 0.03	−2.66 ± 0.009	−2.61 ± 0.02
800	−2.49 ± 0.03	−2.62 ± 0.005	−2.58 ± 0.02

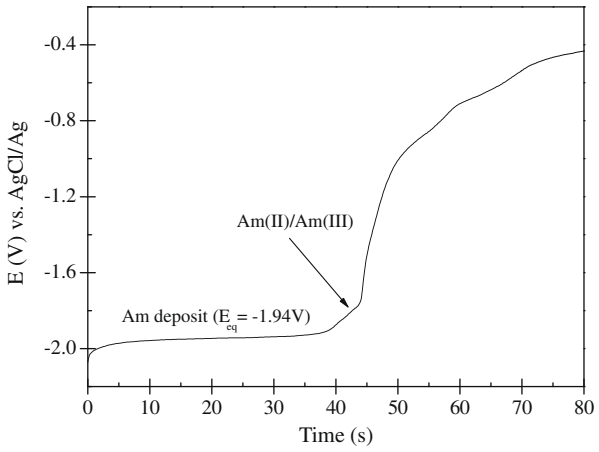

Fig. 4. Open-circuit potential–time curves in $CaCl_2$–NaCl–$AmCl_3$ ([Am] = 0.012 mol/kg) on W (S = 0.29 cm^2). $E_{applied}$ = −2.1 V (360 s). T = 700 °C.

formal standard potential can be calculated from the Nernst equation as follows:

$$E_{eq} = E'^{0}_{Am(II)/Am(0)} \frac{2.3RT}{2F} \log[Am(II)] \quad (8)$$

Nernst equation applied afterwards to the Am(III)/Am(II) system shows that Am(II) ions are largely predominant at the electrode surface.

The potential value obtained is equal to $E'^{0}_{Am(II)/Am(0)}$ = −2.70 V (±10 mV) vs. $Cl_{2(1atm)}/Cl^-$ at 700 °C (mole fraction scale). Table 1 gathers the values obtained at different temperatures. The uncertainty considers the error from the equilibrium potential measurement and the Am concentration variation in the salt phase.

3.3.1.3. Am(III)/Am(0) redox system. The formal standard potential of the Am(III)/Am(0) redox system is calculated by combining those of the Am(III)/Am(II) and Am(II)/Am(0) couples through the Luter's equation: $3E'^{0}_{Am(III)/Am(0)} = E'^{0}_{Am(III)/Am(II)} + 2E'^{0}_{Am(II)/Am(0)}$. The value obtained is $E'^{0}_{Am(III)/Am(0)}$ = −2.64 V (±25 mV) vs. $Cl_{2(1atm)}/Cl^-$ at 700 °C (mole fraction scale). Table 1 indicates the values obtained in the temperature range tested.

3.3.2. Am(III)/Am(Al) formal standard potential

Fig. 5 shows a series of cyclic voltammograms registered in $CaCl_2$–NaCl–$AmCl_3$ at different potential scan rates on liquid Al.

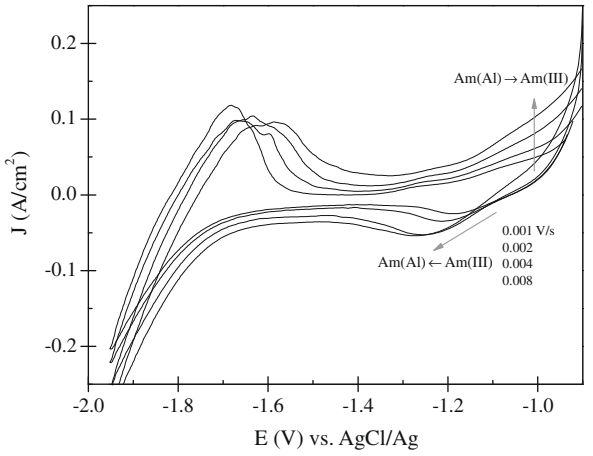

Fig. 5. Cyclic voltammograms of $CaCl_2$–NaCl–$AmCl_3$ ([Am] = 0.0076 mol/kg) on Al(l) (S = 0.37 cm^2) at different potential scan rates. T = 700 °C.

The main characteristics of these curves are the following: (i) the cathodic and anodic peak currents increase with the square root of the scan rate as it can be seen in Fig. 6. This indicates that during the electro-reduction/dissolution processes the reaction is controlled by the diffusion both in the salt and metal phases; (ii) the ratio I_p^A/I_p^C remains close to unity, irrespective of the scan rate. Despite the oxidized Am(III) and reduced Am species are moving in two different media (salt and metal, respectively), the diffusion coefficients in both phases are assumed to be similar; (iii) the E_p^C and E_p^A vary with the logarithm of the potential sweep rate, which indicates the system is not fully reversible.

The formal standard potential of the Am(III)/Am(Al) system has been estimated by using the GPES software to simulate the experimental curves according to a quasi-reversible model. The standard rate constant, the charge transfer coefficient and the formal standard potential were adjusted to get the best fit between the experimental and the calculated results. It has to be indicated that the simulation was focused on the Am(III)/Am(Al) system, i.e., the solvent was not considered. Fig. 7 shows a representative example of the simulation carried out. The value obtained is equal to $E'^{0}_{Am(III)/Am(Al)}$ = −2.21 V (±10 mV) vs. $Cl_{2(1atm)}/Cl^-$ at 700 °C (mole fraction scale).

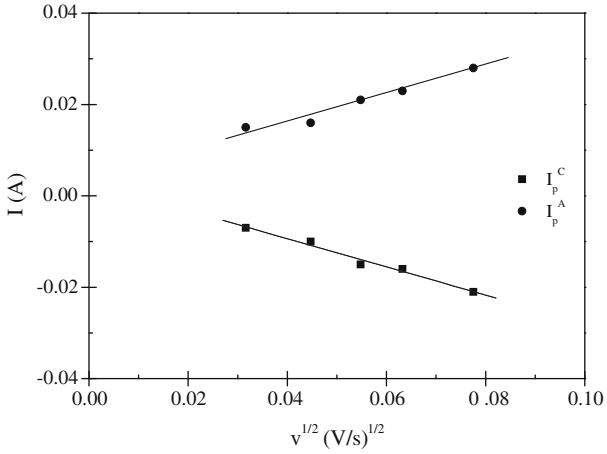

Fig. 6. Variation of the peak current of the Am(III)/Am(Al) redox process as a function of the square root of the scan rate on Al(l) (S = 0.37 cm^2). [Am] = 0.0076 mol/kg. T = 700°C.

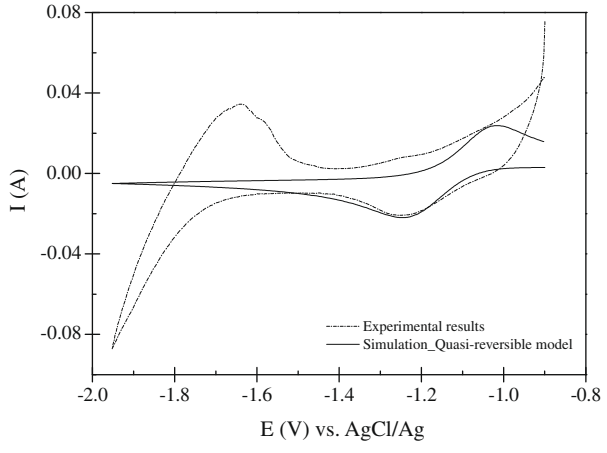

Fig. 7. Cyclic voltammogram of the Am(III)/Am(Al) system on Al(l) (S = 0.37 cm^2) in $CaCl_2$–NaCl. (——) Experimental results; (–) Simulated results according to a quasi-reversible mechanism model (with α = 0.45 and log K = −2.99). v = 0.003 V/s. T = 700 °C.

Table 2
Activity coefficients of Am and Nd in different metallic solvents.

Solvent	T (°C)	$log\ \gamma_{Nd(Me)}$	$log\ \gamma_{Am(Me)}$	$log\ \gamma_{Nd(Me)} - log\ \gamma_{Am(Me)}$
Al	700	−7.80 [10]	−6.7 This work	−1.1
Bi	500	−12.85 [23]	−9.70 [17]	−3.15
Cd	500	−7.94 [24]	−4.10 [17]/−4.68 [21]	−3.8/−3.3

3.3.3. Activity coefficient calculation

The formal standard potentials determined in the preceding Section 3.3.1. and Section 3.3.2. allow the calculation of the logarithm of the activity coefficient through equation (2). The value obtained is equal to $\log\gamma_{Am(Al)} = -6.7$ at 700 °C. An uncertainty on the logarithm of the activity coefficient of ±1 has been estimated. The high working temperature and the low concentration of Am in solution made the analysis of the curves difficult; hence, the value of the activity coefficient is considered as a first approximation.

In the following section, a comparison between different metallic solvents capabilities for the Am/Nd electrolytic extraction is presented.

3.4. Comparison of solvents capabilities

A comparison between the Am and Nd activity coefficients in some metallic solvents, proposed as candidates for the An/Ln separation (Al, Ga, Bi, Zn and Cd), has been intended. In fact, the lack of data on the Am activity coefficient in most of the solvents makes the comparison difficult. To our knowledge, only activity coefficients of Am in Cd and Bi at 450 °C and 500 °C have been published in the literature [17,21]. This study reports an estimation of the activity coefficient of Am in Al(l) at 700 °C. In the case of Nd, the activity coefficients in Al, Ga, Bi, Zn and Cd are known. Therefore, only Al, Cd and Bi phases have been used for the comparison as illustrated in Table 2.

An/Ln separation is controlled by the equilibrium potentials difference between An^{n+}/An and Ln^{n+}/Ln redox couples. By applying the Nernst equation, it is found that the election of a metallic solvent to optimise the separation factor ($S_{An/Ln}$) requires the difference $\log\ \gamma_{Ln(Me)} - \log\gamma_{An(Me)}$ as less negative as possible (see equation (1) in Section 1). According to that, the selectivity of Al at 700 °C for Am/Nd separation would be higher than the one of Bi at 500 °C and this is higher than that of Cd at the same temperature. This result is consistent with those published on the potentialities of Al as candidate for the An/Ln separation [2,8,22].

4. Conclusions

This study has resulted in a first estimation of the activity coefficient of Am in Al(l) ($\log\gamma_{Am(Al)} = -6.7 \pm 1$ at 700 °C) by applying the cyclic voltammetry technique. As the electrolyte, the eutectic $CaCl_2$–NaCl was used. The starting material being an oxide, the Am solution was prepared by direct AmO_2 dissolution by carbochlorination ($Cl_{2(g)} + C_{(s)}$) at 600 °C.

The formal standard potentials of the Am(III)/Am(II) and Am(II)/Am(0) redox systems were obtained in the temperature range 675–800 °C by applying the techniques of cyclic voltammetry and open-circuit chronopotentiometry. Afterwards, the Am(III)/Am(0) formal standard potential was calculated by combining the previous ones.

An "ad hoc" experimental set-up was specifically designed to work with small amounts of solvent and a liquid cathode device. The difficulties encountered by the experimentation with Am yielded a quality of curves not as good as desirable. This fact, attributed to the high working temperature and the low concentration of solute, made their analysis difficult. As a consequence, the reported values for the formal standard potentials and the activity coefficient should be considered approximate.

Acknowledgements

This work has been carried out with the European Commission financial support within the framework of the ACSEPT Collaborative Project (FP7-EURATOM no. 211267). The investigation is also part of the CIEMAT-ENRESA agreement for developing activities in the field of Partitioning and Transmutation. Authors wish to thank the laboratory staff in ATALANTE (Marcoule, CEA) for their technical support.

References

[1] H.P. Nawada, K. Fukuda, J. Phys. Chem. Solids 66 (2005) 647.
[2] O. Conocar, N. Douyère, J.P. Glatz, J. Lacquement, R. Malmbeck, J. Serp, Nucl. Sci. Eng. 153 (2006) 253.
[3] H. Yamana, N. Wakayama, N. Souda, H. Moriyama, J. Nucl. Mater. 278 (2000) 37.
[4] J.P. Ackerman, J.L. Settle, J. Alloy Compd. 199 (1993) 77.
[5] V.A. Lebedev, Selectivity of Liquid Metal Electrodes in Molten Halides, Metallurgiya, Chelyabinsk, 1993.
[6] L. Rault, M. Heusch, M. Allibert, F. Lemort, X. Deschanel, R. Boen, Nucl. Technol. 139 (2002) 167.
[7] O. Conocar, N. Douyère, J. Lacquement, J. Nucl. Mater. 344 (2005) 136.
[8] J. Serp, M. Allibert, A. LeTerrier, R. Malmbeck, M. Ougier, J. Rebizant, J.P. Glatz, J. Electrochem. Soc. 152 (2005) C167.
[9] D.G. Lovering, R.J. Gale, Molten Salt Techniques, vol. 3, Plenum Press, New York, 1987.
[10] G. De Córdoba, A. Laplace, O. Conocar, J. Lacquement, C. Caravaca, Electrochim. Acta 54 (2008) 280.
[11] R.J. Labrie, V.A. Lamb, J. Electrochem. Soc. 106 (1959) 895.
[12] R. Littlewood, Electrochim. Acta 3 (1961) 270.
[13] R.S. Nicholson, I. Shain, Anal. Chem. 36 (1964) 706.
[14] A.J. Bard, L.R. Faulkner, Electrochemical Methods: Fundamental and Applications, second ed., Horwood Publishing, 2001.
[15] D. Lambertin, J. Lacquement, S. Sanchez, G.S. Picard, Plasma Ions 3 (2000) 65.
[16] C. Caravaca, A. Laplace, J. Vermeulen, J. Lacquement, J. Nucl. Mater. 377 (2008) 340.
[17] S.P. Fusselman, J.J. Roy, D.L. Grimmett, L.F. Grantham, C.L. Krueger, J. Electrochem. Soc. 146 (1999) 2573.
[18] J. Serp, P. Chamelot, S. Fourcaudot, R.J.M. Konings, R. Malmbeck, C. Pernel, J.C. Poignet, J. Rebizant, J.P. Glatz, Electrochim. Acta 51 (2006) 4024.
[19] D. Lambertin, S. Sanchez, G.S. Picard, J. Lacquement, Radiochim. Acta 91 (2003) 449.
[20] Y. Castrillejo, M.R. Bermejo, Díaz Arocas, A.M. Martínez, E. Barrado, J. Electroanal. Chem. 579 (2005) 343.
[21] A. Laplace, J. Lacquement, C. Maillard, L. Donnet, in: Nuclear Fuel Cycles for a Sustainable Future, ATALANTE, Nîmes, France, 2004.
[22] A. Laplace, J. Finne, O. Conocar, S. Delpech, J. Vermeulen, L. Blairat, G. Picard, E. Walle, J. Lacquement, in: Proceedings of the Ninth Information Exchange Meeting on Actinide and Fission Product Partitioning and Transmutation, 25–29 September, 2006, Nîmes, France.
[23] M. Kurata, Y. Sakamura, T. Matsui, J. Alloy. Compd. 234 (1996) 83.
[24] Y. Sakamura, T. Inoue, T.S. Storvick, L.F. Grantham, in: Proceedings of the Twenty-sixth Symposium on Molten Salt Chemistry, 1994, Japan Molten Salt Chemical Society, Sapporo (in Japanese).